

# GPR56 promotes proliferation of colorectal cancer cells and enhances metastasis via epithelial-mesenchymal transition through PI3K/AKT signaling activation

BING JI<sup>1\*</sup>, YIFEI FENG<sup>1\*</sup>, YE SUN<sup>2\*</sup>, DONGJIAN JI<sup>1</sup>, WENWEI QIAN<sup>1</sup>, ZHIYUAN ZHANG<sup>1</sup>, QINGYUAN WANG<sup>1</sup>, YUE ZHANG<sup>1</sup>, CHUAN ZHANG<sup>1</sup> and YUEMING SUN<sup>1</sup>

<sup>1</sup>Department of Colorectal Surgery, The First Affiliated Hospital of Nanjing Medical University, Nanjing, Jiangsu 210029; <sup>2</sup>Department of Gastrointestinal Surgery, The First People's Hospital of Changzhou and The Third Affiliated Hospital of Suzhou University, Changzhou, Jiangsu 213003, P.R. China

Received January 11, 2018; Accepted July 17, 2018

DOI: 10.3892/or.2018.6582

**Abstract.** G protein-coupled receptor 56 (GPR56), a member of the orphan GPCR family, has been reported to be an oncogene in various malignancies. However, little is known regarding the detailed molecular mechanism of GPR56 in colorectal cancer (CRC). The present study aimed to detect the expression level and biological function of GPR56 in CRC. We examined the expression of GPR56 in CRC tissues and cell lines by quantitative real time (qRT)-PCR, immunohistochemistry, and western blot analysis. The prognostic significance of GPR56 in CRC patients was evaluated by Kaplan-Meier survival analysis. The influence of GPR56 on tumor cell proliferation (via Cell Counting Kit-8, and a tumor formation assay in mice), apoptosis (flow cytometry), cell cycle distribution (flow cytometry) and migration (Transwell assay) was explored. We also investigated the underlying mechanism of GPR56 by western blot analysis. We found GPR56 expression was significantly upregulated in CRC tissues and cell lines compared to corresponding normal controls. Higher GPR56 expression in patients predicted poorer prognosis. Depletion of GPR56 markedly suppressed cell proliferation, migration, and invasion. GPR56 overexpression promoted CRC cell metastasis by expediting epithelial-mesenchymal transition by activating PI3K/AKT signaling. In conclusion, GPR56 played an important role in CRC progression and may represent a new therapeutic target to reduce CRC metastasis.

## Introduction

Colorectal cancer (CRC) ranks fifth in tumor-related mortality in China and is also considered one of the most common digestive tract malignancies throughout the world (1). CRC poses a growing threat to human health. The lack of effective early diagnosis is of particular concern, since the majority of patients will miss the best opportunity for treatment if they are initially diagnosed at a late stage (2). Thus, it is of great clinical significance to find new early diagnostic markers as well as novel therapeutic targets in CRC to improve patient outcomes.

G protein-coupled receptors (GPCRs) are one of the largest families of membrane proteins, and typically are comprised of a large extracellular domain (ECD), a seven-transmembrane spanning (7TM) domain, and an intracellular domain (ICD) (3). Since more than 30% of drugs currently target GPCRs, it is important to explore and understand their biological function in malignant tumors (4). GPR56, the most studied GPCR in malignant tumors, was first reported to be downregulated in highly metastatic melanoma cell lines compared with poorly metastatic lines by Zendman *et al* in 1999 (5). Since then, research concerning the role of GPR56 in malignancy has covered many aspects, from its differential expression to its mechanism of regulation. Many studies have revealed that GPR56 is expressed as a 3-kb mRNA in various tumor tissues, with higher levels expressed in esophageal squamous cell carcinoma (6), glioblastoma (7), and human fibrosarcoma (8). In terms of its mechanism of action, GPR56 has been implicated in proliferation, migration, angiogenesis, cell adhesion, cell apoptosis, and cell cycle regulation (9-11). It has also been reported that GPR56 plays an important role in several types of malignancies by interacting with vascular endothelial growth factor (VEGF) (11), collagen III (12), CD81 (13), and transglutaminase 2 (Tg2) (14). Furthermore, Jin *et al* recently concluded that GPR56 promoted carcinogenesis by binding progastrin, a pro-angiogenic factor, in mice (15).

Despite the aforementioned studies, the clinical significance and underlying mechanism of action of GPR56 in

---

*Correspondence to:* Dr Yueming Sun, Department of Colorectal Surgery, The First Affiliated Hospital of Nanjing Medical University, 300 Guangzhou Road, Nanjing, Jiangsu 210029, P.R. China  
E-mail: jssunyueming@163.com

\*Contributed equally

**Key words:** GPR56, colorectal cancer, metastasis, epithelial-mesenchymal transition, PI3K/AKT signaling

regulating tumorigenesis and metastasis of CRC remains unclear. Therefore, in this study, we aimed to determine the expression level and biological function of GPR56 in CRC.

## Materials and methods

**Tissue samples and cell culture.** We collected 110 samples of human CRC and corresponding non-tumorous colorectal mucosal tissue between June 2010 and June 2013 at the First Affiliated Hospital of Nanjing Medical University (Nanjing, China). The enrolled patients signed informed consent forms and none had undergone any neoadjuvant radiotherapy or chemotherapy. We snap-froze tissue samples in liquid nitrogen and stored the samples at  $-80^{\circ}\text{C}$  until RNA extraction was performed. The clinicopathological parameters were defined according to The National Comprehensive Cancer Network (2015.2). The Research Ethics Committee of the First Affiliated Hospital of Nanjing Medical University approved this study. We obtained human CRC cell lines (SW480, HT-29, LOVO, DLD-1 and HCT116) and the normal human colorectal epithelial cell line (NCM460) from the American Type Culture Collection (ATCC; Manassas, VA, USA), and cultured the cells in Dulbecco's modified Eagle's medium (DMEM) with 10% fetal bovine serum (FBS; both from Wisent Inc., St-Bruno, Quebec, Canada), 100 U/ml penicillin and 100  $\mu\text{g}/\text{ml}$  streptomycin in a 5%  $\text{CO}_2$  atmosphere at  $37^{\circ}\text{C}$ . We obtained the PI3K inhibitor LY294002 from Cell Signaling Technology (Danvers, MA, USA).

**RNA extraction and qRT-PCR.** Total RNA was isolated from tissues and cells using RNAiso Plus (Takara Biotechnology, Inc., Dalian, China), and cDNA was synthesized using the PrimeScript RT reagent kit (Takara Biotechnology). qRT-PCR was carried out using StepOnePlus Real-time PCR System (Applied Biosystems; Thermo Fisher Scientific, Inc., Foster City, CA, USA) and a SYBR Green PCR kit (Roche Diagnostics, Indianapolis, IN, USA). Specific oligonucleotide primer sequences are listed in Table I. The PCR was performed as follows:  $95^{\circ}\text{C}$  for 30 sec, 40 cycles at  $95^{\circ}\text{C}$  for 5 sec,  $60^{\circ}\text{C}$  for 30 sec; and the dissociation stage at  $95^{\circ}\text{C}$  for 15 sec,  $60^{\circ}\text{C}$  for 1 min and  $95^{\circ}\text{C}$  for 15 sec. The method used for normalizing the qPCR data was the  $2^{-\Delta\Delta\text{Ct}}$  method which facilitates the analysis of relative changes in gene expression in real-time quantitative PCR experiments (16).

**Immunohistochemistry.** Immunohistochemistry was performed as previously described (17). The primary antibody used was GPR56 (diluted 1:200; cat. no. abs133132; Absin Bioscience, Shanghai, China). The total score was calculated based on the percentage of positive cells (0, negative; 1, <30%; 2, 31-60%; 3, >60%) multiplied by the staining intensity (0, negative; 1, weak; 2, moderate; and 3, strong). Scores  $\geq 4$  indicated high GPR56 expression, and scores <4 indicated low GPR56 expression.

**siRNA interference and plasmid transfection.** GenePharma Corp. (Shanghai, China) designed and synthesized the GPR56-targeting small interfering RNAs (siRNAs, si-GPR56) and the negative control siRNAs (si-NC). The GPR56-siRNA sequences were as follows: siRNA1, 5'-GCCUGGUGUUC

UGUUCAATT-3'; siRNA2, 5'-UCACCUCCUCCAAG GCUUTT-3'; and siRNA3, 5'-CCUGGGCCUUGAUCUUCU UTT-3'. The si-NC sequences were as follows: 5'-UUCUCC GAACGUGUCACGUTT-3' (sense) and 5'-ACGUGACAC GUUCGGAGAATT-3' (antisense). The si-GPR56 and si-NC transfection into HCT116 and DLD-1 cells was conducted using Lipofectamine 3000 (Invitrogen; Thermo Fisher Scientific, Inc., Waltham, MA, USA) according to the manufacturer's protocols. After 48 h, knockdown efficiency was evaluated. The GPR56 amplification plasmid was obtained from Sangon Biotech Co., Ltd. (Shanghai, China). The primer sequences were as follows: Forward, 5'-ACGTAGATATATGACTCC CCAGTCGCTGCT-3' and reverse, 5'-ACGTGGTACCGT GCGTTGATCCGGTCCT-3'. The plasmid transfection steps were roughly similar to siRNA interference: A mixture of Opti-MEM, Lipofectamine 3000 and overexpression plasmids prepared in accordance with the instructions were added to a 6-well plate, and the amplification efficiency was ascertained 48 h later.

**Cell proliferation assay.** Cell proliferation was assessed using Cell Counting Kit-8 (Dojindo Molecular Technologies, Tokyo, Japan) assay according to the manufacturer's protocols. Cells ( $2 \times 10^3$  cells/well) were plated in 96-well plates and cultured overnight. Then, 10  $\mu\text{l}$  CCK-8 reagent was added to each well at 24, 48, 72, and 96 h before a 2-h incubation at  $37^{\circ}\text{C}$ . A microplate reader was used to detect the absorbance at 450 nm (test wavelength) and 630 nm (reference wavelength). All experimental procedures were repeated at least three times.

**Mouse tumor xenograft.** Twenty female 4-week-old nude mice (BALB/c nude mice; Vital River, Beijing, China) were purchased from the Laboratory Animal Centre of Nanjing Medical University (Nanjing, China). The specific housing conditions were as follows: Temperature,  $21 \pm 2^{\circ}\text{C}$ ; humidity, 30-70%; 12-h light/dark cycle; the ingested food and water were sterile feed and sterilized bottled water. We selected sixteen mice for our experiments and the average weight of the mice was  $\sim 15$  g. All experimental procedures conducted *in vivo* were in accordance with the guidelines from the Animal Ethical and Welfare Committee of Nanjing Medical University. Cells [HCT116 and DLD-1,  $2 \times 10^6$  cells in 100  $\mu\text{l}$  phosphate-buffered saline (PBS)] were injected into the groins of the nude mice. The mice with tumor implantation were randomly divided into two groups (NC and siRNA) after 4 weeks. Once every 48 h, an intratumoral injection of si-GPR56 or si-NC mixed with the reagent (*in vivo*-jetPEI<sup>®</sup>; Polyplus, New York, NY, USA) was performed according to the manufacturer's instructions. After 4 weeks, the nude mice were sacrificed by cervical dislocation and xenograft tumors were dissected. The volume of the implanted tumors was calculated by using the formula: Volume=(width<sup>2</sup> x length)/2. The maximum tumor volumes were as follows: si-NC (HCT116): 1,456  $\text{mm}^3$ ; si-NC (DLD-1): 1,115  $\text{mm}^3$ ; si-RNA2 (HCT116): 755  $\text{mm}^3$ ; si-RNA2 (DLD-1): 643  $\text{mm}^3$ .

**Flow cytometric analysis.** We detected apoptosis using an Annexin V-FITC Apoptosis Detection kit (BD Biosciences, Franklin Lakes, NJ, USA) according to the

Table I. Primer sequences used for qRT-PCR.

Gene	Forward	Reverse
GAPDH	5'-ACAGTCAGCCGCATCTTCTT-3'	5'-GACAAGCTTCCCGTTCTCAG-3'
GPR56	5'-AGTTCTGGGCCTTTGGCATTCA-3'	5'-AGCACAATGCAAGGCACACAGT-3'

Table II. Analysis of GPR56 expression in colorectal carcinoma and adjacent normal tissues by IHC.

Tissue type	Total scores	No. of samples	$\chi^2$	P-value
Carcinoma	0-3	4	8.286	0.004<0.05
	4-6	16		
Adjacent normal	0-3	13		
	4-6	7		

GPR56 was significantly upregulated in carcinoma tissues than in adjacent normal tissues.

manufacturer's protocols after a 48-h siRNA transfection. The cells were kept on ice and then analyzed by a flow cytometer (Becton-Dickinson, San Jose, CA, USA). The experiment was repeated three times. The HCT116 and DLD-1 cells transfected with si-NC or si-RNA2 were stored for 48 h for cell cycle analysis. Cells were stained with propidium iodide (Sigma-Aldrich; Merck, Darmstadt, Germany) and RNase A (Takara Biotechnology, Dalian, China) for 30 min at room temperature after being fixed with 70% ethanol at -20°C overnight. Assessment of the cell cycle distribution was conducted using flow cytometry (FACSCalibur; BD Biosciences).

**Transwell assay.** Cell migration and invasion were performed in a 24-well Transwell plate with polycarbonate sterile chambers (8  $\mu$ m filters; BD Biosciences) with or without Matrigel coating. Cells were seeded in the upper chamber at a density of  $2 \times 10^4$  cells with 100  $\mu$ l serum-free DMEM, whereas complete culture medium containing 10% fetal bovine serum was added to the lower chamber. After incubation for 24 h at 37°C, we counted the migrated and invaded cells on the membrane using a light microscope and recorded the results as the means  $\pm$  standard deviation (SD). The experiment was performed in triplicate.

**Western blot analysis.** Western blotting was performed as previously described (18). The primary antibodies included were as follows: GPR56 (cat. no. sc-390192), E-cadherin (cat. no. sc-71009), vimentin (cat. no. sc-80975), PI3K (cat. no. sc-293172), AKT (cat. no. sc-135829) and GAPDH (cat. no. sc-47724). These antibodies were purchased from Santa Cruz Biotechnology, Inc., (Dallas, TX, USA) and the dilution ratio was 1:1,000. Secondary antibodies were HRP goat anti-mouse IgG (H+L) (1:5,000; cat. no. 115-035-003; Jackson ImmunoResearch; Shanghai Rebiosci Biotech Co., Ltd., Shanghai, China); p-PI3K (cat. no. 4228) and p-AKT (1:1,000; cat. no. 130308; both from Cell Signaling Technology). Secondary antibodies were goat anti-rabbit IgG (H+L)

(1:5,000; cat. no. 111-035-003; Jackson ImmunoResearch; Shanghai Rebiosci Biotech Co., Ltd.

**Statistical analysis.** Statistical computations were performed using the Statistical Program for Social Sciences (SPSS) 20.0 (IBM Corp., Armonk, NY, USA) and Graph Pad Prism 5.0 software (GraphPad Software, Inc., La Jolla, CA, USA). The Chi-square tests were performed to investigate the associations between GPR56 expression and clinicopathological factors. Differences between the two groups were assessed by Student's t-test, whereas differences between multiple groups were evaluated by one-way ANOVA followed by Student-Newman-Keuls (SNK) post hoc test. Survival data were analyzed using Kaplan-Meier survival curves and log-rank test. Data were expressed as the mean  $\pm$  SD. A P-value <0.05 was considered to indicate a statistically significant difference.

## Results

**GPR56 is overexpressed in CRC and is associated with clinicopathological factors.** First, we assessed the expression of GPR56 by qRT-PCR in 110 pairs of CRC and matched normal adjacent tissues to examine the role of GPR56 in CRC progression. The expression of GPR56 was significantly higher in tumor tissues than adjacent non-tumorous tissues ( $P < 0.001$ ; Fig. 1A). These findings were confirmed by immunohistochemical analysis (Fig. 1B; Table II). Next, we determined the association of GPR56 expression level with the clinicopathological features of patients with CRC (Table III). We divided the 110 pairs of CRC tissue samples into two experimental groups (high,  $n=83$ ; low,  $n=27$ ) based on the mean GPR56 levels. The expression level of GPR56 was significantly associated with the following clinicopathological factors: TNM stage ( $P=0.017$ ), lymph node metastasis ( $P=0.009$ ), depth of invasion ( $P=0.023$ ), and distant metastasis ( $P=0.019$ ). Yet, we found no association between GPR56 levels and other factors, including age ( $P=0.336$ ), sex ( $P=0.322$ ), tumor diameter ( $P=0.224$ ), carcinoembryonic antigen ( $P=0.224$ ), and primary tumor site

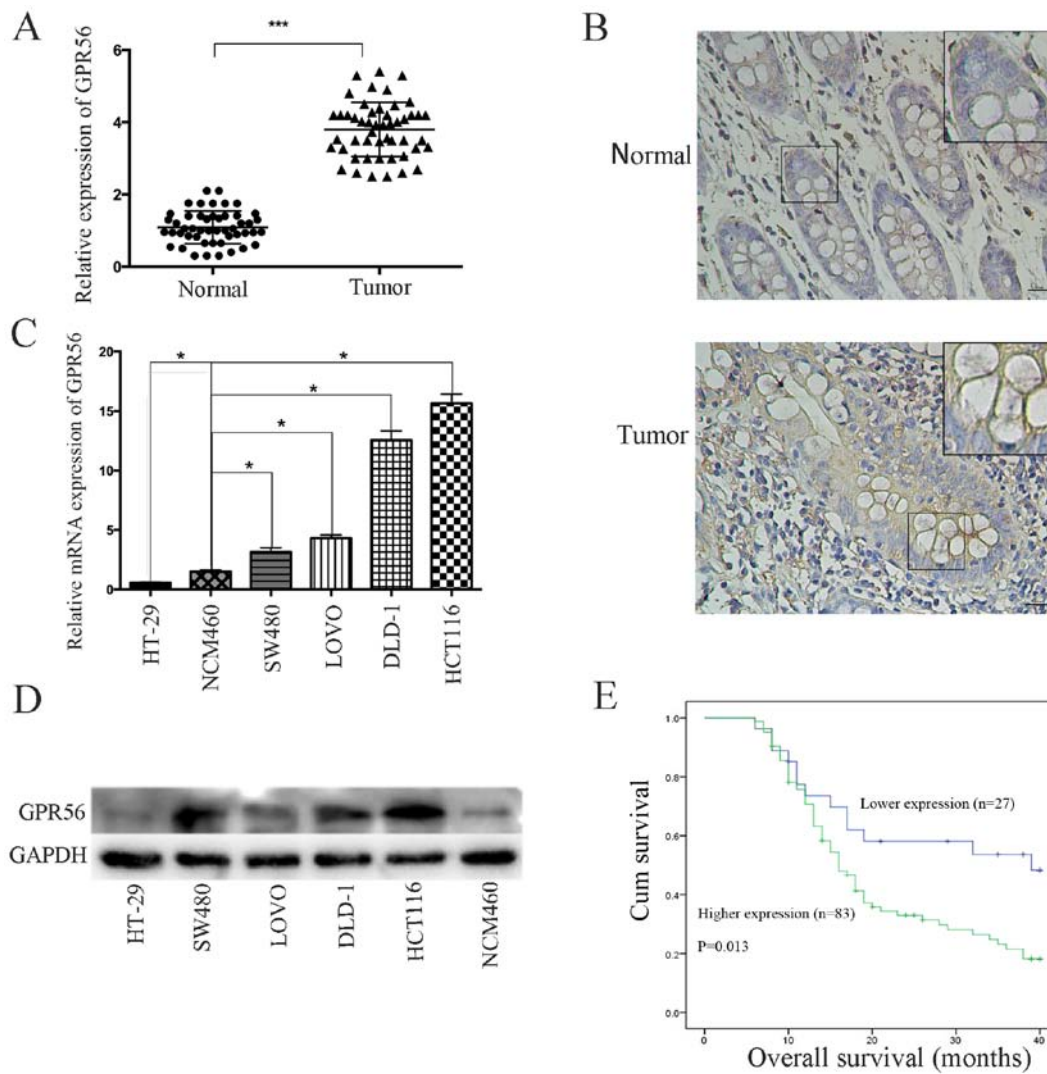


Figure 1. Expression of GPR56 in CRC tissues and cells. (A) The relative expression of GPR56 in 110 pairs of CRC samples by qRT-PCR ( $***P<0.001$ ). (B) The expression of GPR56 protein in CRC samples as determined by immunohistochemistry. (C) The GPR56 expression levels in CRC cell lines in comparison to the normal colorectal epithelial cells (NCM460) by qRT-PCR ( $*P<0.05$ ). (D) The GPR56 protein expression in CRC cell lines and normal colorectal epithelial cells (NCM460) was detected by western blotting. (E) Prognosis of CRC patients divided into high- and low-GPR56 expression groups assessed by Kaplan-Meier overall survival analysis ( $P=0.013$ ).

( $P=0.312$ ). We also examined GPR56 expression levels in CRC cell lines, namely, LOVO, DLD-1, SW480, HT-29, HCT116, and in normal colon epithelial cells (NCM460) by qRT-PCR and western blotting. GPR56 mRNA and protein expression levels were significantly higher in all CRC cell lines apart from HT-29 when compared with NCM460 cells (Fig. 1C and D).

*High expression of GPR56 predicts poor prognosis in patients with CRC.* To further investigate the relationship between GPR56 expression and prognosis of CRC patients, Kaplan-Meier analysis was used to evaluate the correlation between GPR56 expression and overall survival (OS). We found that the OS for patients with low GPR56 levels was significantly better than those with high GPR56 levels ( $P=0.013$ ; Fig. 1E). These data indicated that GPR56 may be helpful for evaluating the prognosis of CRC patients.

*GPR56 knockdown decreases CRC cell proliferation.* We selected the HCT116 and DLD-1 cell lines, which had

higher GPR56 expression levels compared to the other CRC cell lines (LOVO, HT-29, SW480), to examine whether GPR56 levels and cancer cell proliferation were associated. We decreased GPR56 expression levels in the HCT116 and DLD-1 cells using specific siRNA targeting GPR56 (si-RNA1, si-RNA2 and si-RNA3). Cells transfected with si-RNA2 and si-RNA3 had a significantly decreased GPR56 mRNA expression level compared with the negative control (si-NC) group in both cell lines ( $P<0.05$ ; Fig. 2A). Next, we performed Cell Counting Kit-8 (CCK-8) assays to identify the function of GPR56 in the proliferation of CRC cells. We found that cells in which GPR56 was knocked down exhibited decreased proliferation compared to the controls ( $P<0.05$ ; Fig. 2B and C). Since the effect of si-RNA2 was more marked than that of si-RNA3, we only used si-RNA2 in the subsequent experiments. The effects of GPR56 on the cell cycle were further examined via flow cytometry. There were increased cells in the  $G_0/G_1$  phase and decreased cells in the S phase in the GPR56-knockdown group compared

Table III. Association of GPR56 expression with clinicopathological factors in colorectal cancer.

Characteristics	No. of patients	GPR56 expression		P-value <sup>a</sup>
		Low	High	
Age (years)				
<65	49	10	39	0.336
≥65	61	17	44	
Sex				
Male	48	14	34	0.322
Female	62	13	49	
Tumor diameter (cm)				
<5	60	12	35	0.224
≥5	50	15	48	
TNM stage				
I/II	64	21	43	0.017 <sup>a</sup>
III/IV	46	6	40	
Lymph node metastasis				
Positive	44	5	39	0.009 <sup>a</sup>
Negative	66	22	44	
Depth of invasion				
T1+T2	41	15	26	0.023 <sup>a</sup>
T3+T4	69	12	57	
Distant metastasis				
Positive	21	1	20	0.019 <sup>a</sup>
Negative	89	26	63	
CEA				
<4.7	46	14	32	0.224
≥4.7	64	13	51	
Primary tumor site				
Colon	50	10	40	0.312
Rectum	60	17	43	

<sup>a</sup>P<0.05. GPR56, G protein-coupled receptor 56; CEA, carcinoembryonic antigen.

to the controls (Fig. 2D and E). Subsequently, western blot analysis and qRT-PCR were performed to investigate protein and mRNA expression levels of the target proteins associated with the cell cycle distribution (i.e., cyclin D, cyclin E, and c-Myc). We found that protein and mRNA levels of cyclin D, cyclin E, and c-Myc in the control cells (si-NC cells) were higher than in the GPR56-knockdown cells (Fig. 3A and B). To investigate whether GPR56 knockdown could impair tumor formation *in vivo*, HCT116 and DLD-1 cells were injected into the groins of nude mice. After 4 weeks, intratumoral injection with si-GPR56 or si-NC was performed once every 48 h. After 4 weeks, compared with the si-NC group, the tumor weight of the si-RNA2 group exhibited a significant decrease and similar to the results of the *in vitro* cell proliferation experiment, the tumor growth rate was significantly lower in the interfering group (si-RNA2) than in the negative control group (si-NC) (Fig. 3C). In addition, the expression of cell-cycle proteins in tumor tissues formed by

HCT116 in nude mice was detected by western blotting and qRT-PCR. The results revealed that the protein and mRNA levels of cyclin D, cyclin E, and c-Myc in the control mice (si-NC) were higher than in the GPR56-knockdown mice, which was similar with the results of experiment in human colorectal cancer cell lines (Fig. 3D). Collectively, these results indicated that GPR56 played an oncogenic role by stimulating CRC proliferation.

*GPR56 knockdown promotes apoptosis of CRC cells in vitro.* Next, we investigated the association between GPR56 and CRC cell apoptosis by flow cytometry. We found that the cell apoptosis rate was lower in GPR56-knockdown cells than in control cells (si-NC) (i.e., 7.55% vs. 20.74% for the HCT116 cell line; and 10.96%, vs. 32.88% for the DLD-1 cell line). Compared to GPR56-knockdown cells, the rate of apoptosis increased by 13.19% in HCT116 cells and by 21.92% in DLD-1 cells (Fig. 4A and B; P<0.05).

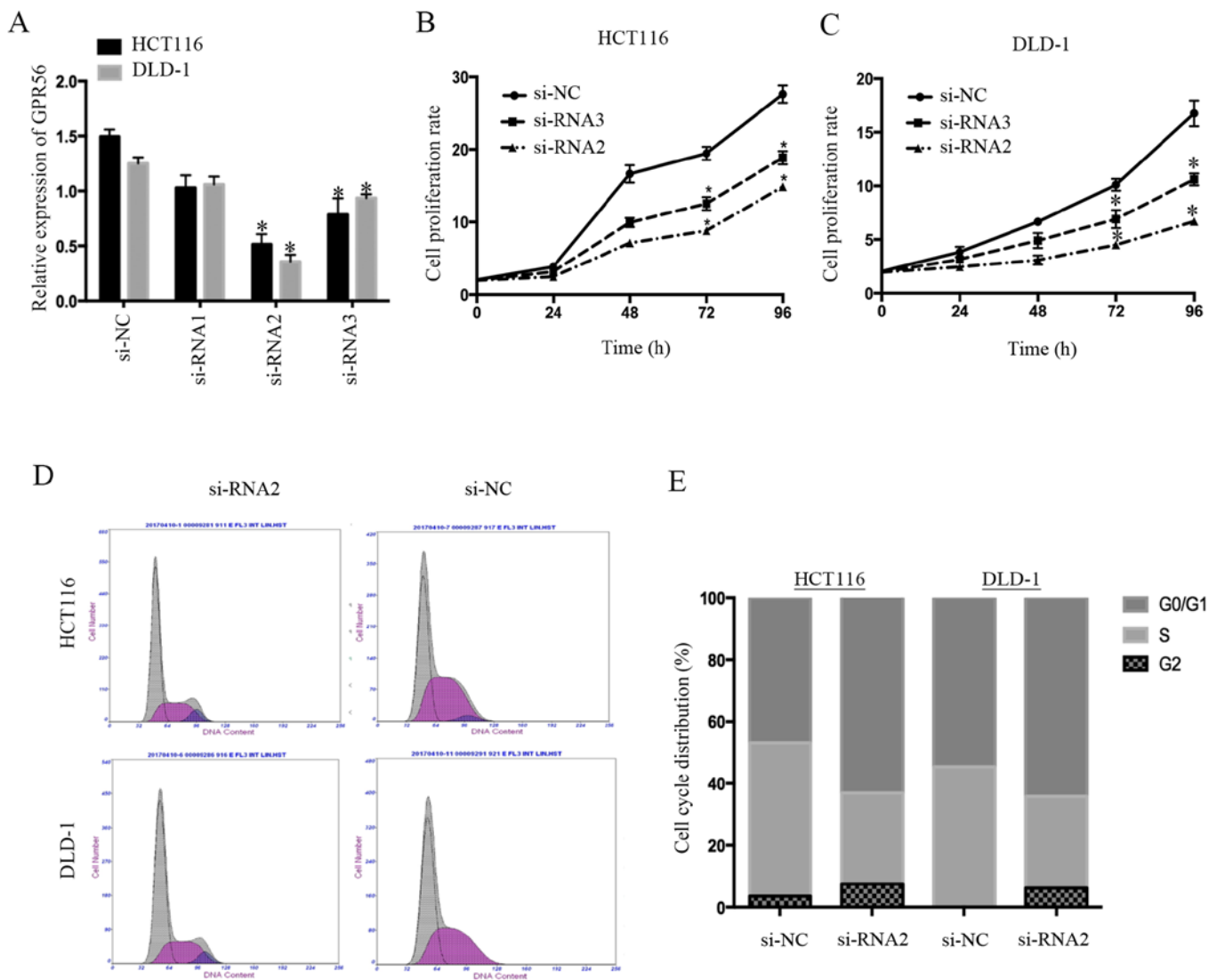


Figure 2. The effect of GPR56 on CRC cell proliferation. (A) The expression of GPR56 was detected by qRT-PCR in HCT116 and DLD-1 cell lines transfected with a negative control (si-NC) and siRNA targeting GPR56 (si-RNA1, si-RNA2, and si-RNA3) ( $P < 0.05$ ). (B and C) A CCK-8 assay revealed that knockdown of GPR56 inhibited cell proliferation in (B) HCT116 and (C) DLD-1 cells ( $P < 0.05$ ). (D and E) The effect of GPR56 knockdown on the HCT116 and DLD-1 cell cycle as assessed by flow cytometry.

Bcl-2 is a known apoptosis inhibitor, while Bax is a pro-apoptotic member of the Bcl-2 family. Therefore, we assessed the expression level of Bcl-2 and Bax proteins in CRC cells (HCT116 and DLD-1) with and without GPR56 knockdown. Western blotting revealed that GPR56 knockdown decreased Bcl-2 levels and increased Bax levels in the HCT116 and DLD-1 cell lines compared to the controls (si-NC) (Fig. 4C). In addition, qRT-PCR analysis of the mRNA expression of Bcl-2 and Bax revealed similar results ( $P < 0.05$ ; Fig. 4D). These results indicated that knockdown of GPR56 activated the apoptosis of CRC cells, possibly by regulating the Bcl-2/Bax ratio.

*GPR56 knockdown inhibits the migration and invasion of CRC cells in vitro.* We performed wound healing and Transwell assays using HCT116 cells and DLD-1 cells to determine the function of GPR56 in CRC cell motility. The wound healing assay revealed a relatively weak migration ability of HCT116 and DLD-1 cells in which GPR56

was knocked down compared to the control group (si-NC) (Fig. 5A). Furthermore, Transwell migration and invasion assays revealed that knockdown of GPR56 significantly inhibited the migration and invasion abilities of both HCT116 and DLD-1 cells (Fig. 5B). Thus, we demonstrated that GPR56 played an important role in the migration and invasion of CRC.

*GPR56 induces epithelial-mesenchymal transition phenotypes.* Epithelial-mesenchymal transition (EMT) is a vital process for primary tumor cells to gain migration ability. We assessed whether GPR56 had any influence on EMT in CRC cells to examine the function of GPR56 in CRC cell proliferation and migration. We determined the protein and mRNA expression levels of E-cadherin, N-cadherin, and vimentin in GPR56-knockdown cell lines compared to the controls (si-NC). We determined that GPR56 knockdown reversed the EMT-related protein levels in both HCT116 and DLD-1 compared to the controls. Specifically, epithelial marker

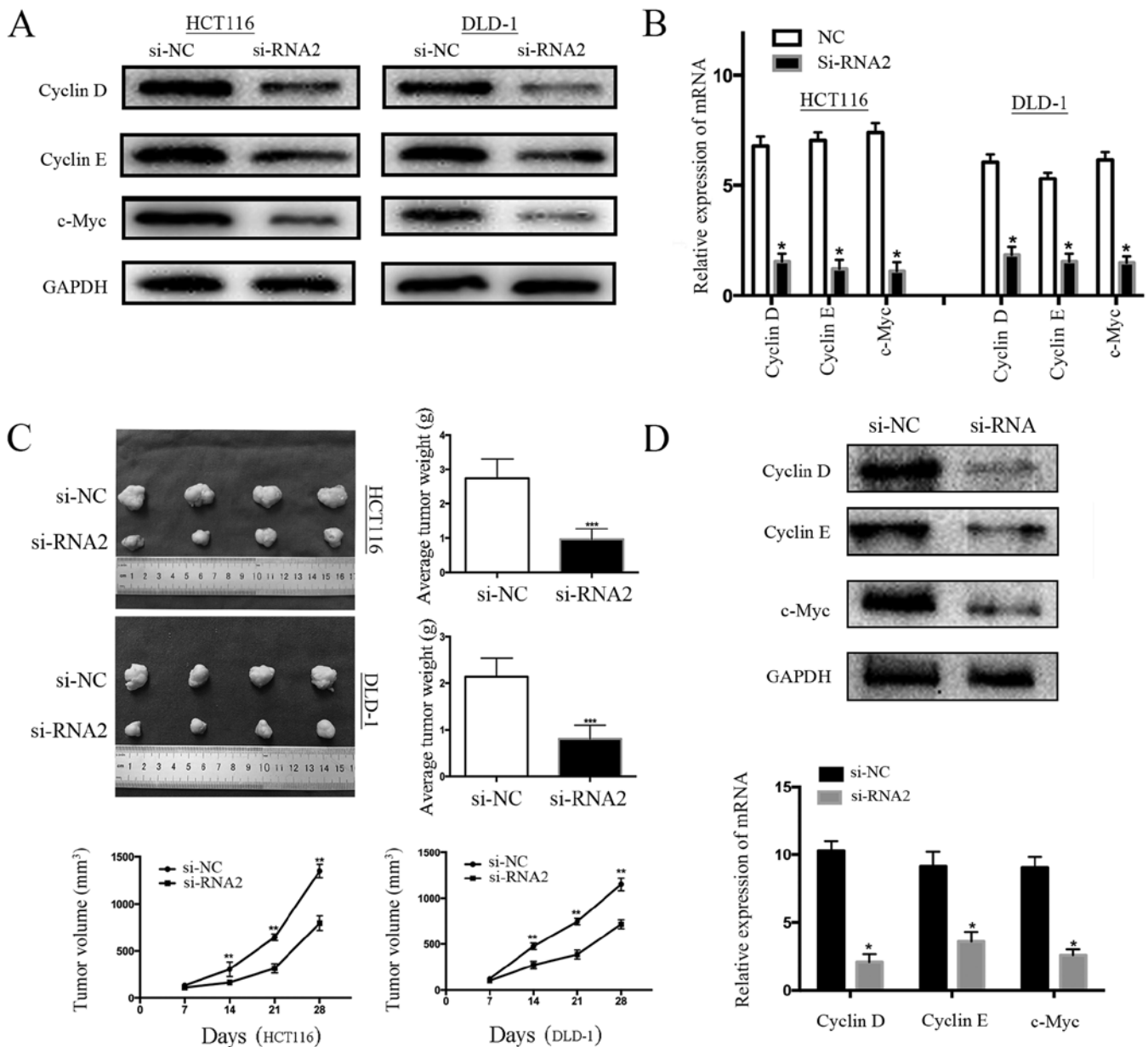


Figure 3. Western blotting results of cell cycle-related proteins and tumor formation experiment *in vivo*. (A) Western blotting and (B) qRT-PCR detection of protein and mRNA expression of cyclin D, cyclin E, and c-Myc; GAPDH was used as a control ( $P < 0.05$ ). (C) Tumors formed by cells (HCT116 or DLD-1) transfected with si-NC (negative control) and si-GPR56 (si-RNA2) were removed by surgery, 4 weeks after cells were injected into the flank of nude mice. The tumor weight was assessed separately ( $***P < 0.001$ ). The growth curve was determined by measuring the tumor volume every 7 days ( $**P < 0.01$ ). (D) Western blotting and qRT-PCR detection of protein and mRNA expression of cyclin D, cyclin E, and c-Myc in tissues formed by HCT116 in nude mice; GAPDH was used as a control ( $P < 0.05$ ).

E-cadherin was highly expressed whereas the expression of the mesenchymal markers N-cadherin and vimentin was significantly decreased (Fig. 5C).

*GPR56 promotes CRC cell migration by inducing EMT via regulation of the PI3K/AKT signaling pathway.* First, we examined the association between GPR56 expression and PI3K/AKT signaling. Western blotting revealed that GPR56 knockdown markedly decreased phosphorylated PI3K and AKT levels but not that of non-phosphorylated PI3K and AKT (Fig. 6A). Considering there are a series of oncogenes reported to promote EMT via activation of the PI3K/AKT signaling pathway in various malignancies, we attempted to uncover

the relationship between the PI3K/AKT signaling pathway and EMT in CRC. We chose the HT-29 cell line, which had a low expression of GPR56, for these experiments and then overexpressed the GPR56-target gene using a special amplification plasmid (Fig. 6B). As predicted, overexpression of GPR56 significantly increased cell migration in a Transwell assay; however, the addition of the PI3K/AKT-specific inhibitor LY294002 decreased the cell migration capacity (Fig. 6C and D).

In addition, western blotting and qRT-PCR analysis revealed that GPR56 overexpression upregulated vimentin and N-cadherin expression and downregulated E-cadherin expression. Conversely, when cells overexpressing GPR56

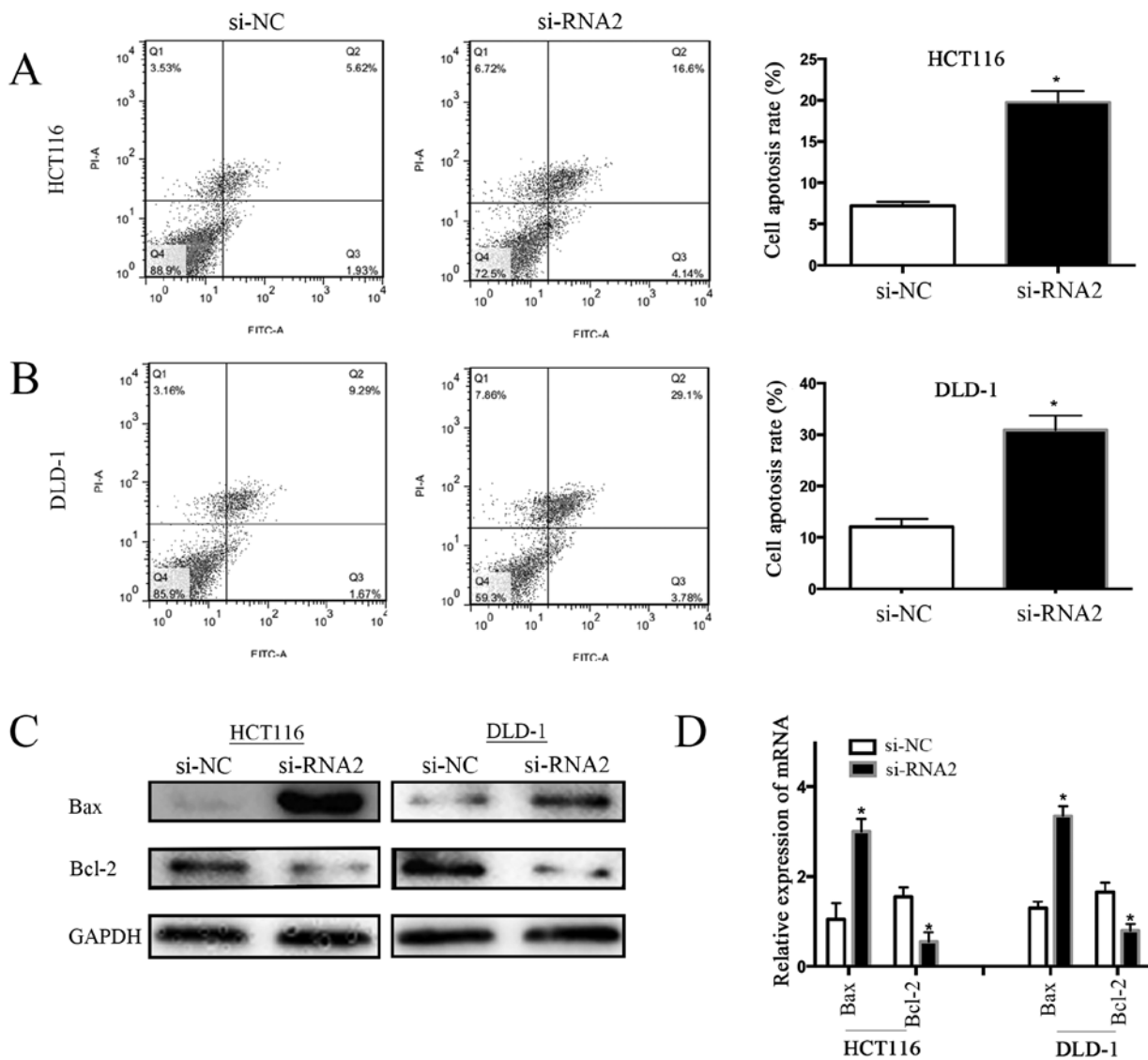


Figure 4. GPR56 knockdown activates apoptosis of CRC cells. Flow cytometry was used to detect the apoptosis of (A) HCT116 and (B) DLD-1 cells ( $P < 0.05$ ). (C) Western blotting and (D) qRT-PCR detection of protein and mRNA expression levels of Bax and Bcl-2 ( $P < 0.05$ ). GAPDH was used as the control.

were treated with LY294002, the typical change in EMT was reversed (Fig. 7A and B). To summarize, these results preliminarily demonstrated that GPR56 promoted EMT via PI3K/AKT signaling, which led to the increased migration ability of CRC cells.

## Discussion

GPCRs have recently become a hot topic in tumor research (19-21). They are reported to be vital regulators of various cellular functions such as cell adhesion, migration, polarity, and guidance. Although the expression of GPR56 has been demonstrated to be increased, decreased, or silenced in either tumor cells or the stromal cells of the tumor micro-environment (22), its precise role and related mechanism in CRC remains unclear. Our study revealed for the first time the GPR56-related regulatory mechanisms that may be involved in the development and metastasis of CRC.

Considering GPR56 was previously found to be upregulated in a series of cancer types [such as esophageal squamous

cell carcinoma, human fibrosarcoma, and human epithelial ovarian cancer (23)], we investigated whether high expression of GPR56 had a similar effect in CRC progression. Our findings indicated that GPR56 was overexpressed at both the mRNA and protein levels in CRC and its high expression was significantly associated with the malignant progression of the primary tumor. We also found that patients with high expression of GPR56 had a relatively poor prognosis compared to those with low expression. These results demonstrated that GPR56 has the potential to be a clinical marker for both diagnosis and prognosis evaluation in CRC.

We also investigated how GPR56 functions as an oncogene in CRC cells. We found that GPR56 played a vital role in changing the proliferation, migration and invasion abilities of CRC cells. GPR56 knockdown also caused CRC cells to arrest at the  $G_0/G_1$  phase and promoted apoptosis in both HCT116 and DLD-1 cell lines. Collectively, our results indicated that high expression of GPR56 was positively associated with the metastatic potential of primary colorectal tumors.



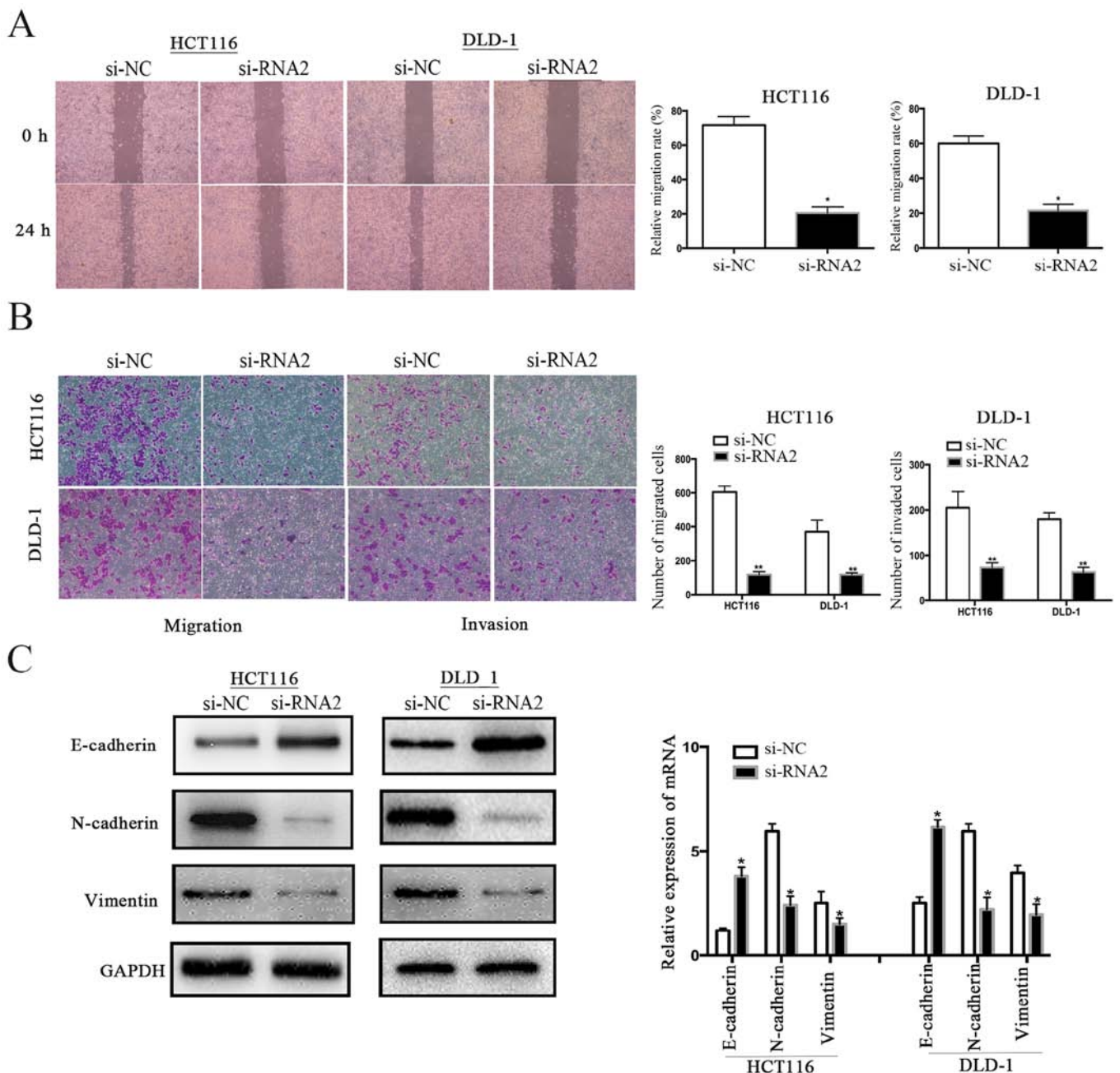


Figure 5. GPR56 knockdown decreases migration and invasion of CRC cells. (A) Wound healing assays revealed the migration rate of HCT116 and DLD-1 CRC cells transfected with a negative control (si-NC) or siRNA targeting GPR56 (si-RNA2). Original magnification,  $\times 40$  ( $P < 0.05$ ). (B) Transwell assays revealed the migration and invasion of HCT116 and DLD-1 CRC cells. Original magnification,  $\times 100$ . Migrated and invaded cells were counted ( $**P < 0.01$ ). (C) GPR56 knockdown in HCT116 and DLD-1 was associated with upregulated E-cadherin and downregulated N-cadherin and vimentin expression; mRNA levels of E-cadherin, N-cadherin, and vimentin were assessed by qRT-PCR ( $P < 0.05$ ).

Since EMT is a vital mechanism in the metastasis of primary cancers (24), we hypothesized that GPR56 may play a role in this process. EMT is a process whereby epithelial cells are transformed into motile mesenchymal cells. It typically occurs during morphogenesis in embryonic development, and is silent in the adult body; however, EMT can be recovered under a variety of pathological conditions, including wound healing, fibrosis, and cancer metastasis (25). Thus, we assessed the expression of EMT-induced markers after knockdown of GPR56 in two CRC cell lines. Depletion of GPR56 evidently weakened N-cadherin and vimentin expression, but increased the expression of E-cadherin. This indicated that GPR56

promoted metastasis of CRC by regulating the expression of genes related to EMT.

The PI3K/AKT signaling pathway is a vital pathway related to cancer progression and invasion (26). Crosstalk between PI3K/AKT signaling and EMT in cancers has been reported (27-30). Thus, we investigated whether PI3K/AKT-mediated EMT was involved in GPR56-mediated migration and invasion in CRC. We determined that overexpression of GPR56 promoted the migration of CRC cells and this promotion could be inhibited by LY294002, a specific inhibitor of PI3K/AKT signaling. Conversely, depletion of GPR56 caused a significant decrease in phosphorylated

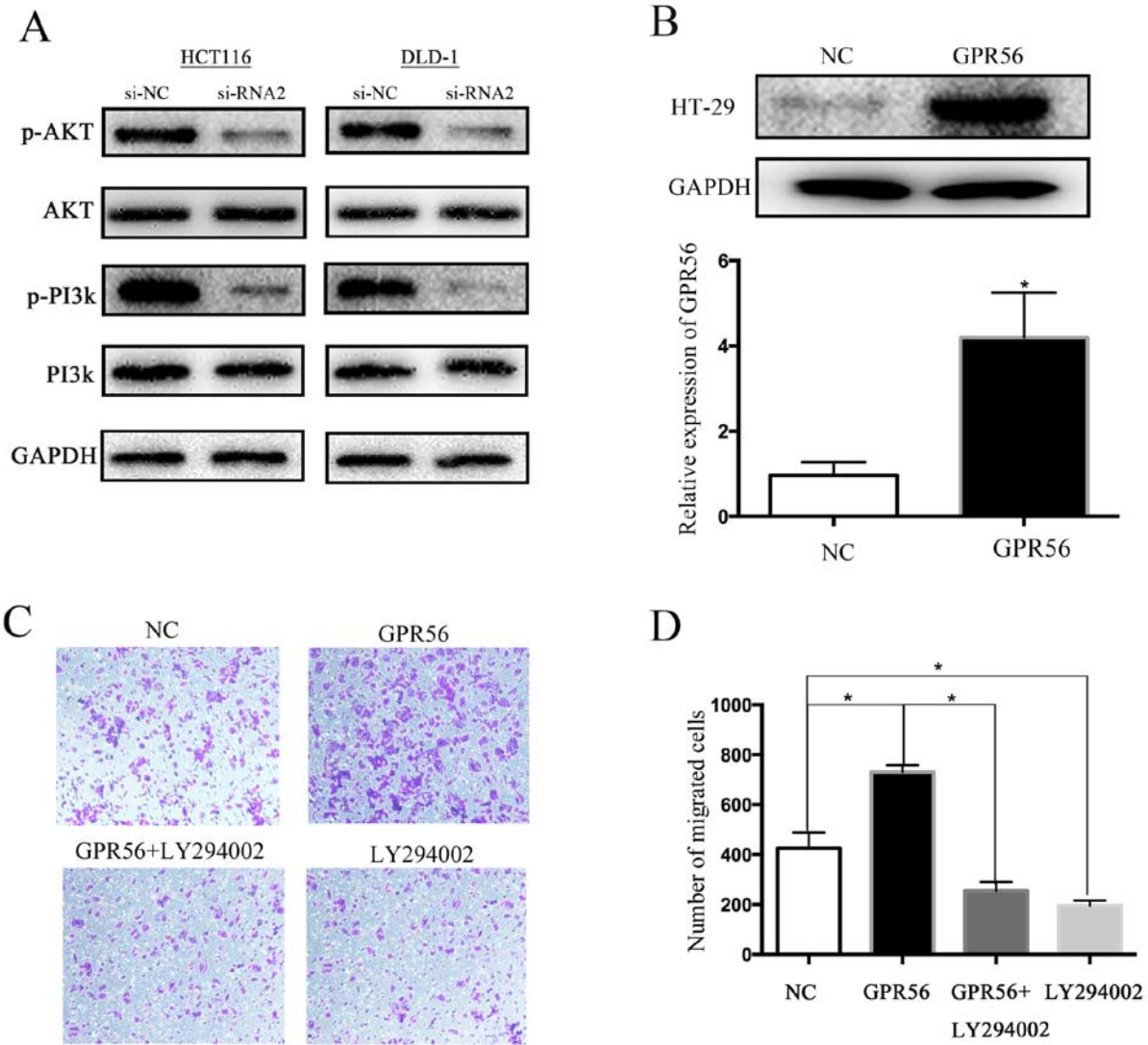


Figure 6. GPR56 impairs cell migration through PI3K/AKT signaling. (A) The expression of p-AKT, AKT, PI3K and p-PI3K was evaluated by western blotting. (B) Western blotting and qRT-PCR of GPR56 protein and mRNA expression, respectively, in HT-29 NC and GPR56-overexpressing cells (GPR56) (\*P<0.05). (C) Transwell migration assays revealed the relationship between GPR56, PI3K/AKT, and CRC cell migration. Magnification, x100. (D) The number of migrated cells were counted (\*P<0.05).

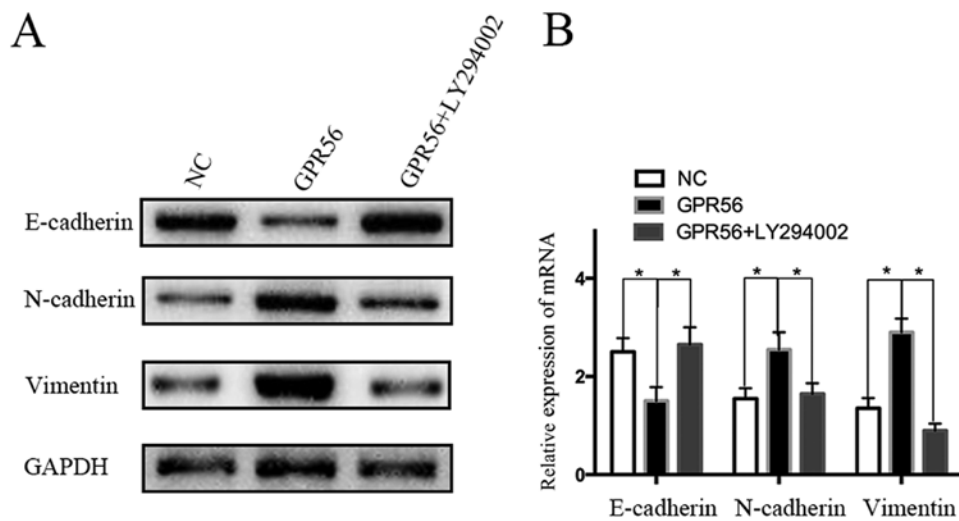


Figure 7. The association between EMT and PI3K/AKT signaling. (A) Western blotting detection of EMT-related target (E-cadherin, N-cadherin and vimentin) proteins and mRNA expression in HT-29 (NC), GPR56-overexpressing cells (GPR56), and GPR56 cells treated with the LY294002 inhibitor (GPR56 + LY294002). (B) qRT-PCR detection of EMT-related target proteins and mRNA (E-cadherin, N-cadherin and vimentin) expression in HT-29 NC and HT-29 with GPR56-overexpressing (GPR56), and GPR56 cells treated with LY294002 (GPR56 + LY294002) (\*P<0.05).

PI3K and AKT. In addition, when cells that expressed high levels of GPR56 were treated with LY294002, EMT was reversed. These observations indicated that high expression of GPR56 affected CRC migration by stimulating EMT via a PI3K/AKT-mediated mechanism.

In conclusion, in the present study, high GPR56 expression was detected in CRC tissues and cell lines at both the protein and mRNA levels. Since GPR56 has an oncogenic role, it has the potential to be a useful biomarker of CRC. Furthermore, GPR56 promoted CRC cell proliferation, migration, and invasion, and was critical in CRC metastasis by stimulating EMT via activation of PI3K/AKT signaling. However, this investigation still has some flaws. We found that GPR56 was highly expressed in most colorectal cancer cell lines (LOVO, DLD-1, SW480, HCT116) but expressed at a relatively low level in HT-29 cells when compared to a normal cell line (NCM460). The molecular mechanism behind this phenomenon remains unclear. We conjectured that it may be related to differences between cell lines and multigene interactions in cancers. The precise underlying mechanism of the interaction between GPR56 and the progression of CRC requires further investigation.

#### Acknowledgements

We thank Hailong Zhao for his assistance with the statistical analysis. We also thank our colleagues at the Public Laboratory of General Surgery, the First Affiliated Hospital of Nanjing Medical University for their technical assistance.

#### Funding

The present study was supported in part by the Jiangsu Key Medical Discipline (General Surgery) (no. ZDXKA2016005).

#### Availability of data and materials

The datasets used during the present study are available from the corresponding author upon reasonable request.

#### Authors' contributions

BJ and YF conceived and designed the study. BJ and YS performed the experiments. BJ wrote the paper. BJ and YF reviewed and edited the manuscript. DJ, WQ, ZZ, QW, YZ and CZ were also involved in the conception of the study and gave their advice in the process of the research. All authors read and approved the manuscript and agree to be accountable for all aspects of the research in ensuring that the accuracy or integrity of any part of the work are appropriately investigated and resolved.

#### Ethics approval and consent to participate

The Research Ethics Committee of the First Affiliated Hospital of Nanjing Medical University approved this study. The enrolled patients signed informed consent forms. All experimental procedures conducted *in vivo* were in accordance with the guidelines from the Animal Ethical and Welfare Committee of Nanjing Medical University.

#### Patient consent for publication

Not applicable.

#### Competing interests

The authors declare that they have no competing interests.

#### References

- Chen W, Zheng R, Baade PD, Zhang S, Zeng H, Bray F, Jemal A, Yu XQ and He J: Cancer statistics in China, 2015. *CA Cancer J Clin* 66: 115-132, 2016.
- Yao H and Zhang Z: Standardized diagnosis and treatment of colorectal liver metastasis. *Zhonghua Wei Chang Wai Ke Za Zhi* 20: 753-757, 2017 (In Chinese).
- Aust G, Zhu D, Van Meir EG and Xu L: Adhesion GPCRs in tumorigenesis. *Handb Exp Pharmacol* 234: 369-396, 2016.
- Drews J: Drug discovery: A historical perspective. *Science* 287: 1960-1964, 2000.
- Zendman AJ, Cornelissen IM, Weidle UH, Ruiter DJ and van Muijen GN: TM7XN1, a novel human EGF-TM7-like cDNA, detected with mRNA differential display using human melanoma cell lines with different metastatic potential. *FEBS Lett* 446: 292-298, 1999.
- Kausar T, Sharma R, Hasan MR, Tripathi SC, Saraya A, Chattopadhyay TK, Gupta SD and Ralhan R: Clinical significance of GPR56, transglutaminase 2, and NF- $\kappa$ B in esophageal squamous cell carcinoma. *Cancer Invest* 29: 42-48, 2011.
- Shashidhar S, Lorente G, Nagavarapu U, Nelson A, Kuo J, Cummins J, Nikolich K, Urfer R and Foehr ED: GPR56 is a GPCR that is overexpressed in gliomas and functions in tumor cell adhesion. *Oncogene* 24: 1673-1682, 2005.
- Mori A, Arai S, Furutani M, Hanaki K, Takeda Y, Moriga T, Kondo Y, Gorrin Rivas MJ and Imamura M: Vascular endothelial growth factor-induced tumor angiogenesis and tumorigenicity in relation to metastasis in a HT1080 human fibrosarcoma cell model. *Int J Cancer* 80: 738-743, 1999.
- Saito Y, Kaneda K, Suekane A, Ichihara E, Nakahata S, Yamakawa N, Nagai K, Mizuno N, Kogawa K, Miura I, *et al*: Maintenance of the hematopoietic stem cell pool in bone marrow niches by EVII-regulated GPR56. *Leukemia* 27: 1637-1649, 2013.
- Chiang NY, Peng YM, Juang HH, Chen TC, Pan HL, Chang GW and Lin HH: GPR56/ADGRG1 activation promotes melanoma cell migration via NTF Dissociation and CTF-mediated  $\alpha$ 12/13/RhoA signaling. *J Invest Dermatol* 137: 727-736, 2017.
- Yang L, Chen G, Mohanty S, Scott G, Fazal F, Rahman A, Begum S, Hynes RO and Xu L: GPR56 Regulates VEGF production and angiogenesis during melanoma progression. *Cancer Res* 71: 5558-5568, 2011.
- Luo R, Jin Z, Deng Y, Strokes N and Piao X: Disease-associated mutations prevent GPR56-collagen III interaction. *PLoS One* 7: e29818, 2012.
- Little KD, Hemler ME and Stipp CS: Dynamic regulation of a GPCR-tetraspanin-G protein complex on intact cells: Central role of CD81 in facilitating GPR56-Gal $\alpha$  q/11 association. *Mol Biol Cell* 15: 2375-2387, 2004.
- Yang L, Friedland S, Corson N and Xu L: GPR56 inhibits melanoma growth by internalizing and degrading its ligand TG2. *Cancer Res* 74: 1022-1031, 2014.
- Jin G, Sakitani K, Wang H, Jin Y, Dubeykovskiy A, Worthley DL, Tailor Y and Wang TC: The G-protein coupled receptor 56, expressed in colonic stem and cancer cells, binds progastrin to promote proliferation and carcinogenesis. *Oncotarget* 8: 40606-40619, 2017.
- Livak KJ and Schmittgen TD: Analysis of relative gene expression data using real-time quantitative PCR and the 2(-Delta Delta C(T)) method. *Methods* 25: 402-408, 2001.
- Wang S, Zhang C, Zhang Z, Qian W, Sun Y, Ji B, Zhang Y, Zhu C, Ji D, Wang Q and Sun Y: Transcriptome analysis in primary colorectal cancer tissues from patients with and without liver metastases using next-generation sequencing. *Cancer Med* 6: 1976-1987, 2017.

18. Sun Y, Ji B, Feng Y, Ji D, Zhu C, Wang S, Zhang C, Zhang D and Sun Y: TRIM59 facilitates the proliferation of colorectal cancer and promotes metastasis via the PI3K/AKT pathway. *Oncol Rep* 38: 43-52, 2017.
19. Kishore A and Hall RA: Disease-associated extracellular loop mutations in the adhesion G protein-coupled receptor G1 (ADGRG1; GPR56) differentially regulate downstream signaling. *J Biol Chem* 292: 9711-9720, 2017.
20. Tseng WY, Jan Wu YJ, Yang TY, Chiang NY, Tsai WP, Gordon S, Chang GW, Kuo CF, Luo SF and Lin HH: High levels of soluble GPR56/ADGRG1 are associated with positive rheumatoid factor and elevated tumor necrosis factor in patients with rheumatoid arthritis. *J Microbiol Immunol Infect* pii: S1684-1182: 30094-30094, 2017.
21. Mehta P and Piao X: Adhesion G-protein coupled receptors and extracellular matrix proteins: Roles in myelination and glial cell development. *Dev Dyn* 246: 275-284, 2017.
22. Ke N, Sundaram R, Liu G, Chionis J, Fan W, Rogers C, Awad T, Grifman M, Yu D, Wong-Staal F and Li QX: Orphan G protein-coupled receptor GPR56 plays a role in cell transformation and tumorigenesis involving the cell adhesion pathway. *Mol Cancer Ther* 6: 1840-1850, 2007.
23. Liu Z, Huang Z, Yang W, Li Z, Xing S, Li H, Hu B and Li P: Expression of orphan GPR56 correlates with tumor progression in human epithelial ovarian cancer. *Neoplasma* 64: 32-39, 2017.
24. Zhang L, Wang X and Lai M: Modulation of epithelial-to-mesenchymal cancerous transition by natural products. *Fitoterapia* 106: 247-255, 2015.
25. Liu PL, Liu WL, Chang JM, Chen YH, Liu YP, Kuo HF, Hsieh CC, Ding YS, Chen WW and Chong IW: MicroRNA-200c inhibits epithelial-mesenchymal transition, invasion, and migration of lung cancer by targeting HMGB1. *PLoS One* 12: e0180844, 2017.
26. Wang SC, Chai DS, Chen CB, Wang ZY and Wang L: HPIP promotes thyroid cancer cell growth, migration and EMT through activating PI3K/AKT signaling pathway. *Biomed Pharmacother* 75: 33-39, 2015.
27. Wei S, Wang L, Zhang L, Li B, Li Z, Zhang Q, Wang J, Chen L, Sun G, Li Q, *et al*: ZNF143 enhances metastasis of gastric cancer by promoting the process of EMT through PI3K/AKT signaling pathway. *Tumour Biol* 37: 12813-12821, 2016.
28. Song Y, Li ZX, Liu X, Wang R, Li LW and Zhang Q: The Wnt/ $\beta$ -catenin and PI3K/Akt signaling pathways promote EMT in gastric cancer by epigenetic regulation via H3 lysine 27 acetylation. *Tumour Biol* 39: 1010428317712617, 2017.
29. Fu H, He Y, Qi L, Chen L, Luo Y, Chen L, Li Y, Zhang N and Guo H: cPLA2 $\alpha$  activates PI3K/AKT and inhibits Smad2/3 during epithelial-mesenchymal transition of hepatocellular carcinoma cells. *Cancer Lett* 403: 260-270, 2017.
30. Xu Q, Liu X, Liu Z, Wang Y, Tu J, Li L, Bao H, Yang L and Tu K: MicroRNA-1296 inhibits metastasis and epithelial-mesenchymal transition of hepatocellular carcinoma by targeting SRPK1-mediated PI3K/AKT pathway. *Mol Cancer* 16: 103, 2017.



This work is licensed under a Creative Commons Attribution-NonCommercial-NoDerivatives 4.0 International (CC BY-NC-ND 4.0) License.